

PETROLOGY OF ZIRCON-BEARING DIOGENITE NORTHWEST AFRICA 10666. T.B. Tanner¹, C.R. Jeffcoat¹, M. Richter¹, E.L. Berger², T.J. Lapen¹, A.J. Irving³, S.M. Kuehner³, G. Fujihara⁴, ¹Department of Earth and Atmospheric Sciences, University of Houston, Houston, TX, USA, ²GCS – Jacobs JETS – NASA Johnson Space Center, Houston, TX, USA, ³Dept. of Earth & Space Sciences, University of Washington, Seattle, WA 98195, ⁴Hilo, HI 96720; Corresponding author: tbanner@uh.edu

Introduction: The howardite, eucrite, and diogenite (HED) meteorites are a group of achondrites thought to be derived from the asteroid 4 Vesta [1], though there is active debate as to whether all diogenites are part of the HED suite [2, 3]. Petrologic investigation of the HED meteorite group provides a means of understanding early planetary differentiation processes and early evolution of planets in our solar system.

Diogenites are predominantly coarse grained orthopyroxenites with some samples containing appreciable amounts of clinopyroxene, olivine, chromite, and plagioclase [2;3]. Accessory metal, troilite, and apatite are common. Many diogenites are brecciated, however, there are few poorly to un-brecciated samples.

Diogenites are important because they may represent the lower crust of 4 Vesta. Although Mg isotope data indicates that the sources of diogenites are ancient [4], their crystallization ages are difficult to constrain due to their protracted thermal histories [5]. The limited chronologic data for diogenites also limits the ability to test petrogenetic connections with eucrites [6] and even parent body. A reliable and high closure-temperature isotope system, such as U-Pb in zircon, is needed to address the timing of diogenite igneous crystallization.

Description of the textures and mineralogy of diogenites are essential to their classification and understanding their formation, in particular, whether all phases are petrogenetically related. Here, we present

detailed petrographic data from a rare zircon-bearing feldspathic diogenite, Northwest Africa (NWA) 10666 and provide textural evidence for igneous crystallization of the zircon.

Analytical Procedures: BSE images and EDX data were obtained using the JEOL JSM 7600 field emission scanning electron microscope at the NASA Johnson Space Center, with accelerating potential = 15kV and current = 30nA. Electron probe microanalyses were performed at the University of Washington.

Petrology: NWA 10666 is medium-grained gabbronoritic diogenite containing 50-60% orthopyroxene that are 1-3 mm in the long dimensions ($\text{Fs}_{35.1-35.2}\text{Wo}_{2.1-1.9}$, $\text{FeO/MnO} = 29$), 20-25% clinopyroxene that are <0.1-0.3 mm ($\text{Fs}_{14.3-14.4}\text{Wo}_{43.5-43.3}$, $\text{FeO/MnO} = 21-24$), 23-25% calcic plagioclase that are 0.5-1 mm ($\text{An}_{81.3}\text{Or}_{3.0}-\text{An}_{86.3}\text{Or}_{0.6}$), 9-10% oxides and sulfides that are <0.1 mm, as well as <1% accessory apatite and zircon that are <0.1 mm. Unlike typical diogenites, this specimen appears poorly brecciated; however, the stone is crosscut extensively with cracks that are filled with an aggregate of fine-grained, Cl-rich phases and silica.

Orthopyroxene defines the dominant orthocumulate texture and occurs as larger, subhedral, interlocking grains. Their composition is more ferroan than plagioclase-poor diogenites [3]. Clinopyroxene exsolution lamellae in orthopyroxene occur variably in nearly

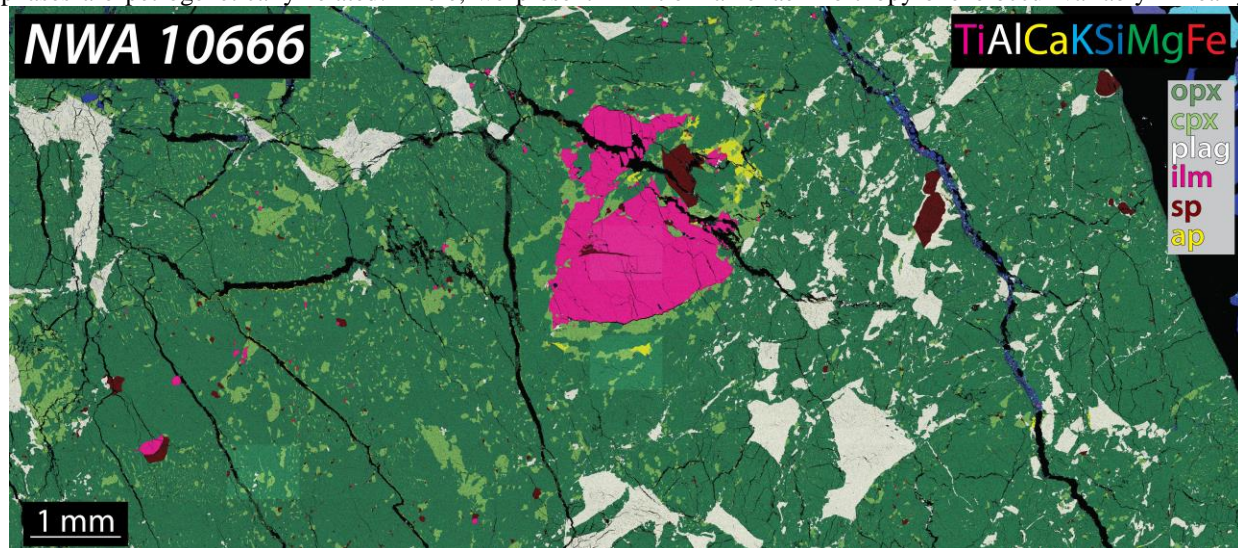


Figure 1: False color composite XRay element map of a portion of NWA 10666.

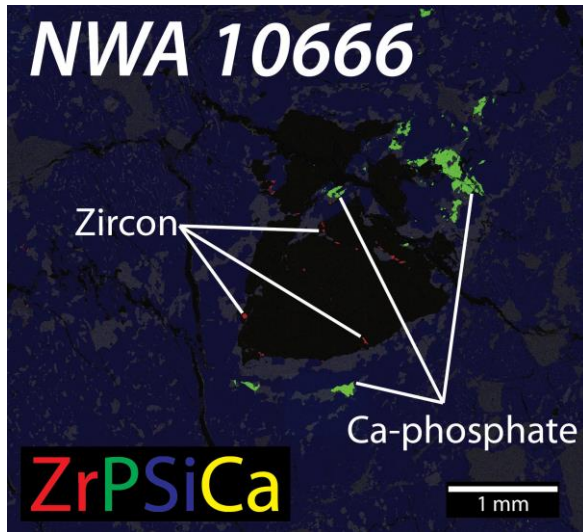


Figure 2: False color composite XRay element map of the large ilmenite grain (black) with guest of zircon (red) and adjacent apatite (green).

all orthopyroxene grains. Areas of orthopyroxene that do not contain well-developed exsolution lamellae are typically associated with larger, irregular-shaped clinopyroxene grains (Figure 1). Less commonly, larger grains of clinopyroxene occur as standalone grains poikilitically enclosed in orthopyroxene and adjacent to the large, interstitial plagioclase and ilmenite grains.

Calcic plagioclase grains are anhedral and irregularly distributed (Figure 1). Grain boundaries between plagioclase and orthopyroxene are locally jagged. Plagioclase also locally occurs surrounding some of the Cr-spinel grains in the plagioclase-rich regions of the sample.

Iron sulfide occurs poikilitically enclosed in orthopyroxene and some clinopyroxene. Iron sulfide is in highest abundance in areas where calcic plagioclase is

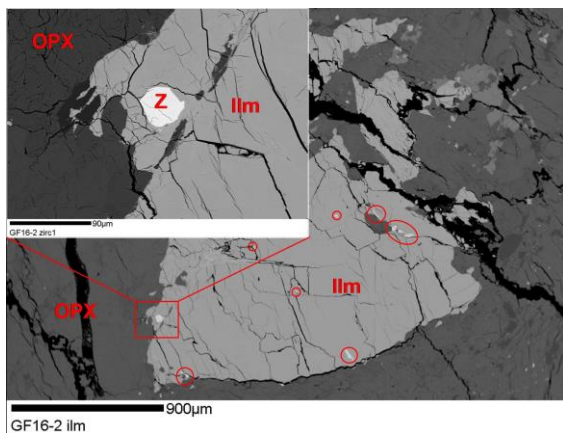


Figure 3: BSE image of the large ilmenite grain hosting zircon.

least abundant. A large grain (3-4 mm) of ilmenite hosts several (>15) grains of zircon that are euhedral to subhedral. Ilmenite also occurs as small spherical grains (<0.1mm) locally associated with Cr-spinel.

Apatite grains (Figure 2) are predominately present adjacent to discrete clinopyroxene grains and occur mostly near the large ilmenite grain in the sample (Figure 1). Zircon grains (Figure 2 and 3) are present exclusively as inclusions in and on the boundary of the large ilmenite grain. Cr-spinel grains are bimodally distributed (<0.1mm; 4mm) and are present as anhedral to subhedral equant grains. Iron sulfide grains occur as spherical grains (<0.1mm).

Discussion: Textural and mineralogical associations indicate that the large orthopyroxene was an early forming phase. The ilmenite that hosts the zircons appears to be intergrown in an igneous, not fracture contact with the host orthopyroxene and clinopyroxene. The compositions of the pyroxene in the plagioclase-rich areas are compositionally identical to the pyroxenes in the plagioclase poor areas suggesting that these areas are not likely a mixture of distinct lithologies. As yet, there is no evidence that the zircons are unrelated to the host diagenetic lithology.

The zircons contained in NWA 10666 represent the first recognized occurrence of this datable phase in a diogenite. The zircons are large enough for *in situ* analysis of U-Pb isotope compositions and Ti-in-zircon thermometry [7]. The phosphate grains are also amenable to U-Pb dating, but have a lower closure temperature than zircon (e.g. >1000°C for Pb diffusion in zircon to ~ 550°C for Pb diffusion in apatite [8;9]). Coupled zircon and apatite age analysis in concert with thermal modeling based on Ti in zircon thermometry and closure temperature calculations based on grain size may constrain the reliability of the zircon U-Pb ages as a record of igneous crystallization of this diogenite sample.

References: [1] McSween H. Y. et al. (2011) *Space Science Reviews*, 163, 141–174. [2] Irving A. et al. (2014) 77th *Meteorit. Soc. Mtg.*, #5199 [3] Irving A. et al. (2016) *LPS XLVII*, #2264 [4] Schiller M et al. (2011) *Geochim. Cosmochim. Acta.*, 74, 4844-4864. [5] McSween H. Y. et al. (2013) *Meteorit. & Plant. Sci.*, 48, 2019-2104. [6] Takahashi K. and Masuda K. (1990) *Nature*, 343, 540-542. [7] Watson E. B. et al. (2006) *Contrib. Mineral. Petrol.*, 151, 413-433. [8] Chamberlain K. R. and Bowring S. A. (2000) *Chemical Geology*, 172, 173-200. [9] Cherniak D. J. (2010) *Reviews in Mineralogy and Geochemistry*, 72, 827-869.